Preparation of aligned $Ca_3Co_2O_6$ nanorods and their steplike magnetization

P. L. Li, X. Y. Yao, F. Gao, C. Zhao, K. B. Yin, Y. Y. Weng, and J.-M. Liu[a)]
Laboratory of Solid State Microstructures, Nanjing University, Nanjing 210093, China and International Center for Materials Physics, Chinese Academy of Sciences, Shenyang 110016, China

Z. F. Ren
Department of Physics, Boston College, Chestnut Hill, Massachusetts 02467

(Received 5 June 2007; accepted 3 July 2007; published online 27 July 2007)

Well-aligned $Ca_3Co_2O_6$ nanorods (~300 nm in length and ~40 nm in diameter) on Si substrates are prepared by pulsed laser deposition. The steplike magnetization feature as identified in bulk $Ca_3Co_2O_6$ can be retained in the nanorods in spite of the enhanced distortion of the magnetically ordered spin chains due to the finite size effect. The out-of-plane magnetization value is slightly larger than the in-plane value, which shows the small magnetic anisotropy. An additional distinct transition at 54 K associated with the spin frustration is revealed, different from the bulk samples. © *2007 American Institute of Physics*. [DOI: 10.1063/1.2764443]

Low-dimensional materials are currently in the limelight because of their fundamental and technological significance.[1,2] Among these materials, one-dimensional compounds belonging to the family with the general formula A'_3ABO_6 (A' is Ca or Sr, while A and B are transition metal elements) have received attentions recently. As the only compound of this class in which both A and B sites are identical, $Ca_3Co_2O_6$ has attracted great interest.[1–13] For example, a large magnetoresistance (MR) effect was evidenced in $Ca_3Co_2O_6$ single crystals with the MR value reaching up to 80% at 2 K,[4] while a high thermoelectric efficiency at high temperature (1300 K) was observed.[5] Subsequently, the same behavior was confirmed in polycrystalline ceramic $Ca_3Co_2O_6$.[6]

The crystal structure of $Ca_3Co_2O_6$ is composed of parallel one-dimensional (1D) Co_2O_6 chains built by successive alternating face-sharing CoO_6 trigonal prisms and CoO_6 octahedra along the hexagonal c axis, separated by Ca^{2+} ions. On the a-b plane each chain is surrounded by six equally spaced chains, constituting a hexagonal arrangement. The interchain interaction along the c axis is ferromagnetic (FM) and the intrachain interaction in the a-b plane is antiferromagnetic (AFM), and the FM coupling is much stronger than that of the interchain coupling.[1,2] In fact, subsequent investigations into the nature of magnetism in $Ca_3Co_2O_6$ did reveal highly anisotropic spin configuration and fascinating spin frustrating behaviors, with which interesting phenomena such as FM order, AFM order, and more complex multistate coexistence, were associated.[1,2,7–13] Among these properties, the step magnetization (step-M) as a function of external magnetic field H at low temperature T has been paid attention.[11–13] This step-M behavior shows weak hysteresis feature and features the high stability of saved data against fluctuations of H, which is an advantage in realistic data storage applications.

The increase of magnetic storage density may be limited in future by the size-related instability.[14] In order to overcome this limit, alternative materials and approaches are being pursued. One of the possible approaches may be the step-M behavior observed in $Ca_3Co_2O_6$ as mentioned above. However, no results on thin film processing of $Ca_3Co_2O_6$ have been reported so far, in particular, upon an integration with Si-based integrated circuit technologies. It is our challenge to search for a kind of materials which retain a high step-M stability when the materials size is down to nanoscale, and at the same time to develop a processing roadmap with which the nanoscale materials can be synthesized in an aligned manner. Considering the interesting properties of $Ca_3Co_2O_6$, it is meaningful to fabricate aligned $Ca_3Co_2O_6$ nanorods.

In this work, we prepare $Ca_3Co_2O_6$ nanorod films on single-crystal Si (100) substrates by pulsed laser deposition (PLD). The $Ca_3Co_2O_6$ ceramic target was prepared by a solid-state method.[7] The laser wavelength, pulse width, pulse frequency, and energy density were 248 nm, 30 ns, 5 Hz, and ~2 J/cm^2, respectively. The deposition was performed under an oxygen pressure of 10 Pa and the substrate temperature was 800 °C. After deposition, the samples were *in situ* annealed under the same condition (800 °C, 10 Pa) for 10 min, and then slowly cooled down to room temperature in 0.5 atm of oxygen. The crystallization and morphology of the $Ca_3Co_2O_6$ were investigated by x-ray diffraction (XRD), scanning electron microscopy (SEM), and transmission electron microscopy (TEM). The magnetization (M) as a function of T and H was measured using superconducting quantum interference device magnetometer. All the M-H curves were measured under quasistatic field condition, with the equivalent field variation rate of ~0.003 T/s.

Figure 1(a) shows the XRD spectra of the as-prepared $Ca_3Co_2O_6$ nanorod films directly deposited on (100) Si. All the diffraction peaks can be indexed according to $Ca_3Co_2O_6$ and no diffraction peak from impurity phases is identified. In contrast to the XRD spectra of bulk $Ca_3Co_2O_6$ powder [Fig. 1(b)], reflections (300), (110), and (410) are suppressed and (113) and (214) are the strongest peaks, indicating the slight c-axis preference of the nanorods. The lattice parameters of $Ca_3Co_2O_6$ nanorods are a=0.902 nm and c=1.036 nm, similar to bulk $Ca_3Co_2O_6$ (a=0.907 nm and c=1.038 nm).[1] In Fig. 2, the cross-sectional TEM and SEM images of the $Ca_3Co_2O_6$ nanorod film are shown. Figure 2(a) gives the TEM image, and the image of a single

[a)]Author to whom correspondence should be addressed; electronic mail: liujm@nju.edu.cn

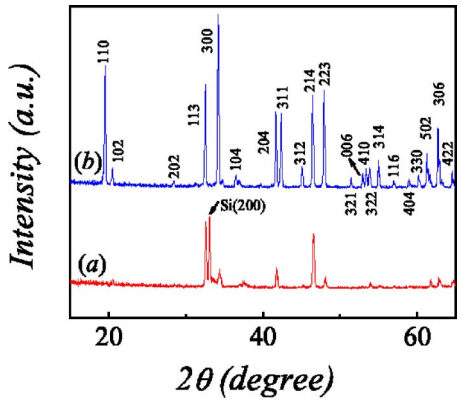

FIG. 1. (Color online) XRD pattern of (a) $Ca_3Co_2O_6$ nanorods on Si substrate and (b) the bulk $Ca_3Co_2O_6$.

nanorod taken from Fig. 2(a) is given in Fig. 2(b). It is seen that the $Ca_3Co_2O_6$ nanorods are about 300 nm in length and 40 nm in diameter in an aligned pattern with conic tips. This view is consistent with the SEM image [Fig. 2(f)]: homogeneous dots of ~40 nm in diameter correspond to the horizontal projection of $Ca_3Co_2O_6$ nanorods. Further reduction of the rod diameter is possible by functioning the deposition time and temperature.

We demonstrate that each nanorod in the film is a single crystal although the film as a whole is polycrystallized. A representative nanorod is shown in Fig. 2(b) and the high-resolution TEM images taken from the three different rectangle regions are given in Figs. 2(c)–2(e). The nanorod tip is

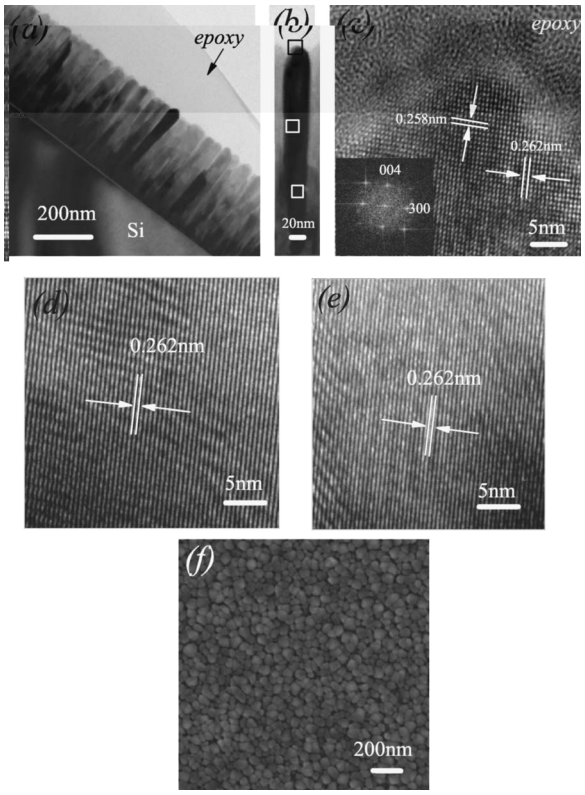

FIG. 2. (a) Cross-sectional TEM image of the nanorod film. (b) TEM image of a single nanorod. [(c)–(e)] HRTEM images of the top, middle, and bottom regions as labeled by the rectangular areas in (b) for this nanorod, respectively. The inset of (c) is the fast Fourier transform image of a selected area, and the white background is caused by the epoxy. (f) SEM top-view image of $Ca_3Co_2O_6$ nanorods film.

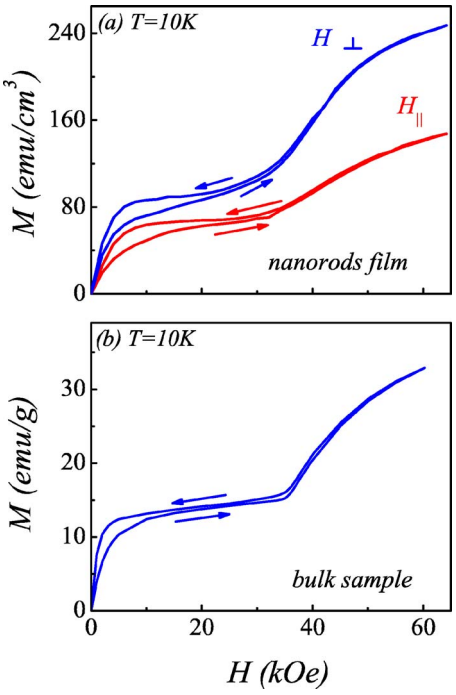

FIG. 3. (Color online) M as a function of H at 10 K for (a) $Ca_3Co_2O_6$ nanorods with H parallel (in plane) and perpendicular (out of plane) to the Si substrate and (b) $Ca_3Co_2O_6$ bulk. The arrows mark the path of the measurement. Data are corrected for the diamagnetism of the Si substrate.

cuspidal, and the interplanar spacings are 0.258 and 0.262 nm, corresponding to the (004) and (300) planes. The same lattice structure and orientation are also illustrated in Figs. 2(d) and 2(e), indicating that this rod is a single crystal. The same identification was performed for the other rods. Furthermore, the $Ca_3Co_2O_6$/Si interfacial region is an amorphous layer of ~5 nm in thickness.

The step-M effect is available in the aligned $Ca_3Co_2O_6$ nanorod film. With H parallel (in plane) and perpendicular (out of plane) to the Si substrate, the in-plane and out-of-plane M vs H are evidenced in Fig. 3(a). For a comparison, we also measured the step-M behavior of bulk $Ca_3Co_2O_6$ sample [Fig. 3(b)]. The $Ca_3Co_2O_6$ nanorod film demonstrates the clean step-M behavior and the height and width of the step are roughly similar to those for the bulk sample. Moreover, as shown in Fig. 3(a), the out-of-plane magnetization is only slightly larger than the in-plane value, indicating the small magnetic anisotropy. For the nanorod film, as H increases, the step appears at $H \sim 0.7$ T and retains until $H \sim 2.8$ T (out of plane), over which M goes up sequentially. For the bulk sample, the step appears at $H \sim 1.0$ T and retains until $H \sim 3.6$ T, consistent with earlier reports.[1,2,9] In addition, the hysteresis is available but not very significant for both the nanorod film and bulk sample, indicating relatively weak dynamic relaxation of the spin-frustrating configuration. Therefore, one is allowed to conclude that the step-M effect can be retained upon reduction of the nanorod diameter down to ~40 nm.

The step-M effect for $Ca_3Co_2O_6$ is well explained in earlier literature[1,2,9,11,12] and no details will be given here. We concentrate on the size dependence of this effect. Previous investigations on bulk $Ca_3Co_2O_6$ indicated that the step-M behavior may be suppressed owing to the breaking or disordering of the spin chains, as confirmed by experiments on chromium site selective substitution in $Ca_3Co_2O_6$ due to the

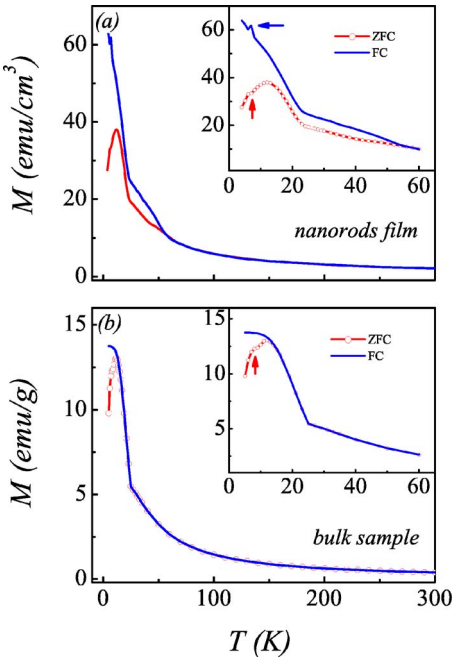

FIG. 4. (Color online) M as a function of T under $H=10$ kOe for (a) $Ca_3Co_2O_6$ nanorods and (b) $Ca_3Co_2O_6$ bulk. The arrows indicate the transitions at (a) 7 K and (b) 8 K.

weakened intrachain FM coupling.[9] The Monte Carlo simulation revealed the disorder-induced significant suppression of the step-M effect.[13] For the $Ca_3Co_2O_6$ nanorod, it is expected that the intrachain FM and interchain AFM couplings are weaker than those of the bulk due to the breaking or disordering of the spin chains from the dimension reduction and relaxation of spins on the large surface. Considering what mentioned above, we can argue that upon reduction in the diameter of the nanorods the magnetization step will be suppressed completely. This issue still warrants for future exploration.

It is also important to investigate the T dependence of the dc magnetizations of the $Ca_3Co_2O_6$ nanorod films under zero field cooling (ZFC) and field cooling (FC), which was performed under a constant $H=10$ kOe, as shown in Fig. 4(a). For the ZFC case the sample is paramagnetic when T goes from 300 down to ~25 K, below which a rapid increasing of M with decreasing T is identified. This corresponds to a ferrimagnetic transition due to the interchain AFM coupling and the spin-frustrated structure.[2,8] Further reduction of T leads to a peak at ~12 K, indicating a transition from the ferrimagnetic order to an inhomogenous state.[8] Also, as the arrows marked in the inset of Fig. 4(a), an additional shoulder at $T\sim7$ K is observed, which may be an indication of the frozen spin state.[2,8] These features are roughly consistent with our data on the bulk sample with the additional shoulder at $T\sim8$ K, as shown in Fig. 4(b), in agreement with earlier reports.[1,2,4,7] Nevertheless, some delicate difference between the nanorod film and bulk sample should be mentioned here. Under the same dc magnetic field ($H=10$ kOe), the bifurcation of the ZFC and FC curves for the $Ca_3Co_2O_6$ nanorod film occurs at $T\sim54$ K, much higher than that of the bulk sample (at $T\sim12$ K). The phenomenon may reveal that the spin frustration for the nanorod film sample appears at $T\sim54$ K, while this transition does not occur until $T\sim12$ K for the bulk sample.[7,9] We also find that for the nanorods there is a peak at ~7 K in the FC curve, which corresponds to the additional shoulder in the ZFC curve. The nature of this shoulder feature is not clear at present. The differences between $Ca_3Co_2O_6$ nanorod film and bulk sample indicate that the spatial dimension plays a key role on the magnetism.

Conventional magnetic storage materials require high magnetocrystalline anisotropy and high coercivity, including CoCr-based alloys and FePt duality alloys.[14] Using $Ca_3Co_2O_6$ nanorods as potential memory media, the level step plays the key role. In addition, as an especial material, $Ca_3Co_2O_6$ nanorods have some advantages in technical preparation. For one thing, $Ca_3Co_2O_6$ nanorods can be achieved on Si substrate without difficulty, and for the other, the steplike behavior kept well though $Ca_3Co_2O_6$ nanorods are polycrystalline on the whole. It is worth pointing out that, among the spin-frustrated systems, $Ca_3Co_2O_6$ is not the only compound which exhibits step-M behavior.[15]

In summary, $Ca_3Co_2O_6$ nanorod films on Si substrates were fabricated by PLD method. The steplike magnetization is observed clearly though it is less defined compared to the bulk, indicating the distortion of the magnetically ordered spin chains. The ZFC-FC curves reveal the typical spin-glass behavior associated with the spin frustration. The out-of-plane and in-plane magnetization curves (for nanorods films) were observed, indicating the small magnetic anisotropy. The present work may shed lights for magnetic storage applications using $Ca_3Co_2O_6$ nanorods and other compounds with spin-frustrated structures due to the property of multistep magnetization.

This work was supported by the National Natural Science Foundation of China (50332020, 50528203, and 50502018) and National Key Projects for Basic Research of China (2002CB613303, and 2006CB921802).

[1] H. Fjellvag, E. Gulbrandsen, S. Aasland, A. Olsen, and B. C. Hauback, J. Solid State Chem. **124**, 190 (1996); S. Aasland, H. Fjellvag, and B. Hauback, Solid State Commun. **101**, 187 (1997).
[2] H. Kageyama, K. Yoshimura, K. Kosuge, H. Mitamura, and T. Goto, J. Phys. Soc. Jpn. **66**, 1607 (1997); A. Maignan, C. Michel, A. C. Masset, C. Martin, and B. Raveau, Eur. Phys. J. B **15**, 657 (2000).
[3] K. Boulahya, M. Parras, and J. M. G-Calbet, J. Solid State Chem. **145**, 116 (1999).
[4] B. Raquet, M. N. Baibich, J. M. Broto, H. Rakoto, S. Lambert, and A. Maigna, Phys. Rev. B **65**, 104442 (2002).
[5] M. Mikami, R. Funahashi, M. Yoshimura, Y. Mori, and T. Sasaki, J. Appl. Phys. **94**, 6579 (2003).
[6] A. Maignan, S. Hébert, C. Martin, and D. Flahaut, Mater. Sci. Eng., B **104**, 121 (2003).
[7] S. Rayaprol, K. Sengupta, and E. V. Sampathkumaran, Solid State Commun. **128**, 79 (2003).
[8] V. Hardy, S. Lambert, M. R. Lees, and D. Mck. Paul, Phys. Rev. B **68**, 014424 (2003); X. Y. Yao, S. Dong, H. Yu, and J.-M. Liu, *ibid.* **74**, 134421 (2006).
[9] D. Flahaut, A. Maignan, S. Hebert, C. Martin, R. Retoux, and V. Hardy, Phys. Rev. B **70**, 094418 (2004).
[10] V. Hardy, M. R. Lees, O. A. Petrenko, D. M. Paul, D. Flahaut, S. Hébert, and A. Maignan, Phys. Rev. B **70**, 064424 (2004).
[11] X. Y. Yao, S. Dong, and J.-M. Liu, Phys. Rev. B **73**, 212415 (2006).
[12] Y. B. Kudasov, Phys. Rev. Lett. **96**, 027212 (2006).
[13] X. Y. Yao, P. L. Li, S. Dong., and J.-M. Liu, Fron. Phys. China **2**, 88 (2007).
[14] S. H. Sun, C. B. Murray, D. Weller, L. Folks, and A. Moser, Science **287**, 1989 (2000).
[15] E. V. Sampathkumaran and Asad Niazi, Phys. Rev. B **65**, 180401 (2002).